NATIONAL TECHNICAL UNIVERSITY OF ATHENS (NTUA)
SCHOOL OF MECHANICAL ENGINEERING
LAB. OF THERMAL TURBOMACHINES
PARALLEL CFD & OPTIMIZATION UNIT (PCOpt/NTUA)

Theoretical Background of the Continuous Adjoint Method in OpenFOAM, incl. Applications

Dr. Kyriakos C. Giannakoglou, Professor NTUA

Dr. E.M. Papoutsis-Kiachagias

November 9, 2022, 42 slides

PCOpt/NTUA: Research Pillars, Personnel, Funding, Comp. Infrastructure

Gradient-based Shape Optimization (ShpO) in CFD

Flow Model (CFD S/W).

Shape Parameterization Technique,
→ Design Variables (Degrees of Freedom, DoFs): b_n, n=1,…,N.

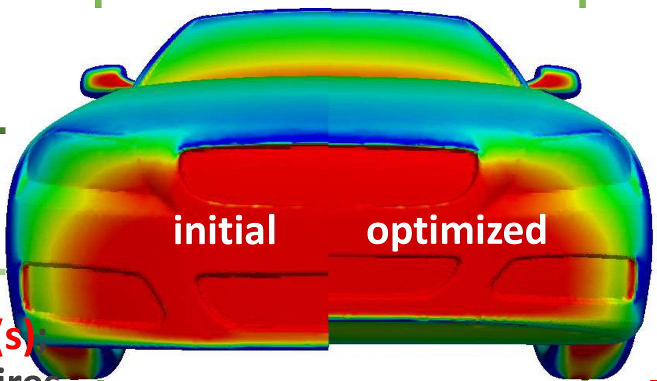

Objective & Constraint Function(s):
gradient-based optimization requires their derivatives w.r.t. b_n, n=1,…,N.

Optimization Method, using gradients computed by the Adjoint Method!

OpenFOAM

All implemented within OpenFOAM v2206:
"adjointOptimisationFoam"
No need for third-party software, external scripts, etc

The Adjoint Method in Optimization Algorithms

Used to compute the gradient of the objective function J (or constraint functions c) w.r.t. the design variables b_n, n=1,…,N, in a problem governed by PDEs (such as the Navier-Stokes eqs.) and drive a descent method towards the optimal solution or just compute Sensitivity Maps.

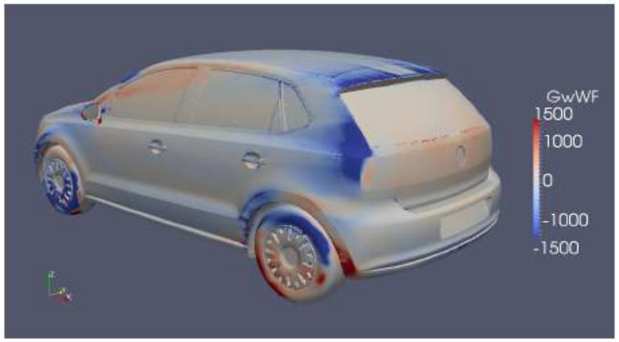

Sensitivity map of downforce of the VW Polo car, computed by *adjointOptimisationFoam*.
Red : move inwards; blue : outwards for better traction to the ground.

Application funded by

The Sensitivity Map is a plot of the iso-areas of the derivative of J w.r.t. the normal displacement of points on the surface to be optimized and signifies the contribution of each part of the body surface, if deformed, to the improvement in J. It helps the designer to make decisions and take actions.

Outline

Part 1: **Understanding Continuous Adjoint using a Quasi-1D Flow Problem (Inverse Design of an Axisymmetric Duct)**

Part 2: **Extension of the Continuous Adjoint to Multi-Dimensional & Turbulent Flows –Shape Optimization (ShpO) – Capabilities of *adjointOptimisationFoam* – Industrial Applications**

Part 3: **Additional Capabilities of the "in-house" OpenFOAM Adjoint Solver**

Part 1:
The Adjoint Method –
Understanding Continuous Adjoint using a Quasi-1D Flow Problem (Inverse Design of an Axisymmetric Duct)

Inverse Design of a Quasi-1D Duct – Incompressible Flow

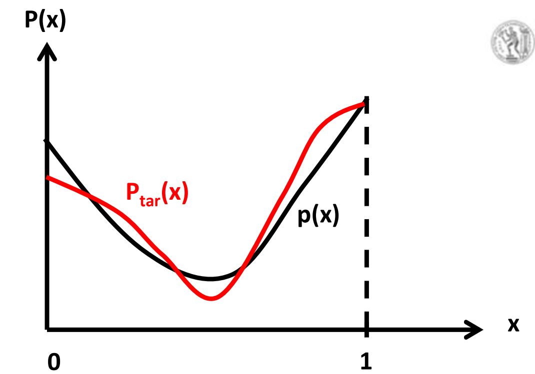

Objective Function (min.):

$$J = \frac{1}{2}\int_0^1 \left(p(x) - p_{tar}(x)\right)^2 dx$$

Shape (Cross-Sectional Area) Parameterization:

$$S(x, b_1, b_2, b_3, b_4) = b_1 + b_2 x + b_3 x^2 + b_4 x^3$$

Design/Optimization Variables:

$$b_n, \; n = 1, 2, 3, 4$$

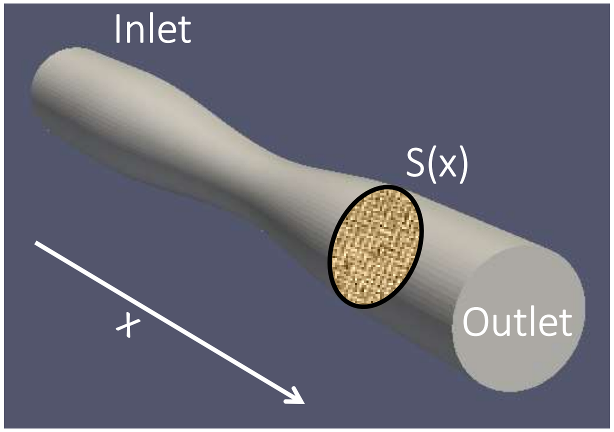

State/Primal/Flow Equations (ODEs):

$$\frac{d(vS)}{dx} = 0 \qquad v\frac{dv}{dx} + \frac{dp}{dx} = 0$$

State/Primal/Flow Boundary Conditions:

$$v|_{x=0} = v_0 \qquad p|_{x=1} = p_0$$

Inverse Design of a Quasi-1D Duct – Incompressible Flow

Differentiate the objective function w.r.t. b_n:

$$\frac{\delta J}{\delta b_n} = \int_0^1 (p(x) - p_{tar}(x)) \frac{\delta p}{\delta b_n} dx, \;\; n=1,...,N$$

Differentiate the flow (primal or state) equations:

$$\left. \begin{array}{l} S\frac{d}{dx}\left(\frac{\delta v}{\delta b_n}\right) + \frac{dS}{dx}\frac{\delta v}{\delta b_n} + \frac{dv}{dx}\frac{\delta S}{\delta b_n} + v\frac{d}{dx}\left(\frac{\delta S}{\delta b_n}\right) = 0 \\ \frac{\delta v}{\delta b_n}\frac{dv}{dx} + v\frac{d}{dx}\left(\frac{\delta v}{\delta b_n}\right) + \frac{d}{dx}\left(\frac{\delta p}{\delta b_n}\right) = 0 \end{array} \right\} \; n=1,...,N$$

Differentiate the flow (primal or state) BCs:

$$\left.\frac{\delta v}{\delta b_n}\right|_{x=0} = 0, \quad \left.\frac{\delta p}{\delta b_n}\right|_{x=1} = 0$$

DD: Direct Differentiation
(cost scales with N)

Adjoint is the art of computing $\frac{\delta J}{\delta b_n}$ without first computing $\frac{\delta v}{\delta b_n}$ and $\frac{\delta p}{\delta b_n}$.

Inverse Design of a Quasi-1D Duct – Incompressible Flow

Define & differentiate the augmented objective function or Lagrangian of J:

$$L = J + \int_0^1 q \frac{d(vS)}{dx} dx + \int_0^1 u \left[v \frac{dv}{dx} + \frac{dp}{dx} \right] dx$$

$$\frac{\delta L}{\delta b_n} = \frac{\delta J}{\delta b_n} + \int_0^1 q \frac{d}{dx} \left[\frac{\delta (vS)}{\delta b_n} \right] dx + \int_0^1 u \left[\frac{\delta v}{\delta b_n} \frac{dv}{dx} + v \frac{d}{dx} \left(\frac{\delta v}{\delta b_n} \right) + \frac{d}{dx} \left(\frac{\delta p}{\delta b_n} \right) \right] dx$$

where q and u are the adjoint pressure and velocity (1D) fields.
Integrate by parts:

$$\frac{\delta L}{\delta b_n} = -\int_0^1 \left[-u \frac{dv}{dx} + \frac{d(vu)}{dx} + S \frac{dq}{dx} \right] \frac{\delta v}{\delta b_n} dx + \int_0^1 \left(-\frac{du}{dx} + p - p_{tar} \right) \frac{\delta p}{\delta b_n} dx$$
$$- \int_0^1 v \frac{dq}{dx} \frac{\delta S}{\delta b_n} dx + \left[(vu + qS) \frac{\delta v}{\delta b_n} \right]_{x=0}^{x=1} + \left[u \frac{\delta p}{\delta b_n} \right]_{x=0}^{x=1} + \left[vq \frac{\delta S}{\delta b_n} \right]_{x=0}^{x=1}$$

Inverse Design of a Quasi-1D Duct – Incompressible Flow

Adjoint field eqs.:

$$\frac{du}{dx} = p - p_{tar} \qquad u\frac{dv}{dx} - \frac{d(vu)}{dx} - S\frac{dq}{dx} = 0 \quad \left(\text{or} \;\; v\frac{du}{dx} + S\frac{dq}{dx} = 0 \right)$$

Adjoint BCs:

$$u|_{x=0} = 0, \quad q|_{x=1} = -\left.\frac{vu}{S}\right|_{x=1}$$

<u>Compare</u> with the primal (flow) problem equations & boundary conditions:

$$\frac{d(vS)}{dx} = 0 \qquad v\frac{dv}{dx} + \frac{dp}{dx} = 0$$

$$v|_{x=0} = v_0 \qquad p|_{x=1} = p_0$$

Inverse Design of a Quasi-1D Duct – Incompressible Flow

Sensitivity Derivatives (SDs):

$$\frac{\delta L}{\delta b_n} = \frac{\delta J}{\delta b_n} = -\int_0^1 v \frac{dq}{dx}\frac{\delta S}{\delta b_n} dx + vq\frac{\delta S}{\delta b_n}\bigg|_{x=1} - vq\frac{\delta S}{\delta b_n}\bigg|_{x=0}, \quad n=1,\ldots,4$$

or:

$$\frac{\delta J}{\delta b_1} = -\int_0^1 v\frac{dq}{dx}dx + vq|_{x=1} - vq|_{x=0}$$

$$\frac{\delta J}{\delta b_2} = -\int_0^1 v\frac{dq}{dx}x\,dx + vq|_{x=1}$$

$$\frac{\delta J}{\delta b_3} = -\int_0^1 v\frac{dq}{dx}x^2 dx + vq|_{x=1}$$

$$\frac{\delta J}{\delta b_4} = -\int_0^1 v\frac{dq}{dx}x^3 dx + vq|_{x=1}$$

(**since:** $S(x,b_1,b_2,b_3,b_4) = b_1 + b_2 x + b_3 x^2 + b_4 x^3$)

Optimization Methods once gradient have been computed

Steepest descent:

$$\vec{b}^{k+1} = \vec{b}^{k} - \eta \left.\frac{\delta J}{\delta \vec{b}}\right|^{k}$$

or Quasi-Newton methods (BFGS, LBFGS, DBFGS, SR1):

$$\vec{b}^{k+1} = \vec{b}^{k} + \Delta\vec{b}, \qquad \Delta\vec{b} = -H^{-1}\frac{\delta J}{\delta \vec{b}} \qquad\qquad (H \approx \delta^2 J/\delta \vec{b}^2)$$

(for the computation of the Exact Hessian matrix see papers cited below).
or the Conjugate Gradient method.

For Constrained Optimization: SQP and Constraint Projection.

►All available in *adjointOptimisationFOAM*.

International Journal for Numerical Methods in Fluids, 56(10):1929-1943, 2008.
Computers & Fluids, 37:1029-1039, 2008.
International Journal for Numerical Methods in Fluids, Vol. 68(6):724-739, 2012.

Inverse Design of a Quasi-1D Duct – Incompressible Flow

Cross Section

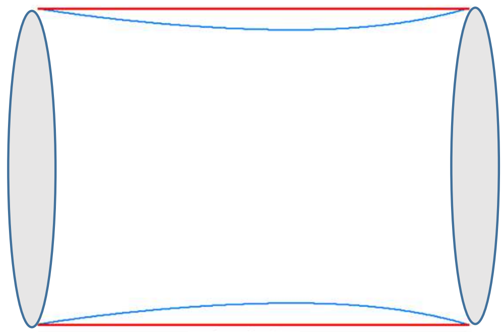

$$J = \frac{1}{2}\int_0^1 \left(p(x) - p_{tar}(x)\right)^2 dx$$

Target Duct

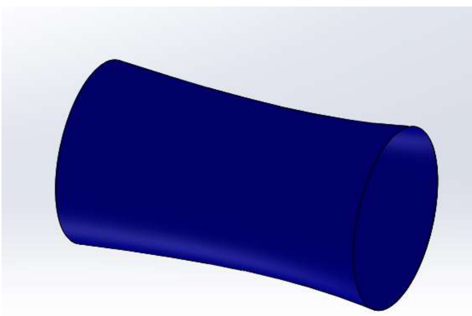

Pressure

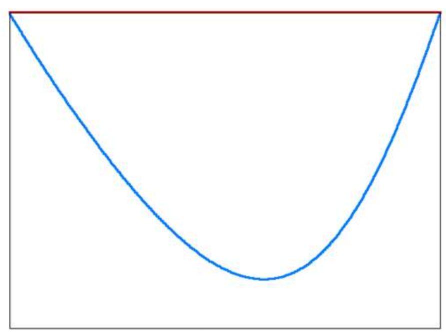

Convergence History

Prof. K.C. Giannakoglou, kgianna@mail.ntua.gr, Dr. E. Papoutsis-Kiachagias, vaggelisp@gmail.com

From Continuous to Discrete Adjoint

Minimize $F = F(\overrightarrow{U}(\overrightarrow{b}), \overrightarrow{b})$

Subject to $\overrightarrow{R} = \overrightarrow{R}(\overrightarrow{U}(\overrightarrow{b}), \overrightarrow{b}) = 0$

Both in discrete form

Compute $$\frac{\delta F}{\delta \overrightarrow{b}} = \frac{\partial F}{\partial \overrightarrow{b}} + \frac{\partial F}{\partial \overrightarrow{U}} \frac{\delta \overrightarrow{U}}{\delta \overrightarrow{b}}$$

Subject to $$\frac{\delta \overrightarrow{R}}{\delta \overrightarrow{b}} = \frac{\partial \overrightarrow{R}}{\partial \overrightarrow{b}} + \frac{\partial \overrightarrow{R}}{\partial \overrightarrow{U}} \frac{\delta \overrightarrow{U}}{\delta \overrightarrow{b}} = 0$$

This is the computationally demanding part!
(*Cost scales with N*)

From Continuous to Discrete Adjoint

Adjoint variables

$$\frac{\delta F_{aug}}{\delta \vec{b}} = \frac{\partial F}{\partial \vec{b}} + \frac{\partial F}{\partial \vec{U}}\frac{\delta \vec{U}}{\delta \vec{b}} - \vec{\Psi}^T \left(\frac{\partial \vec{R}}{\partial \vec{b}} + \frac{\partial \vec{R}}{\partial \vec{U}}\frac{\delta \vec{U}}{\delta \vec{b}} \right)$$

$$\frac{\delta F_{aug}}{\delta \vec{b}} = \frac{\partial F}{\partial \vec{b}} - \vec{\Psi}^T \frac{\partial \vec{R}}{\partial \vec{b}}$$

$$\frac{\partial F}{\partial \vec{U}} - \vec{\Psi}^T \frac{\partial \vec{R}}{\partial \vec{U}} = 0$$

Adjoint equation

Compare:
Discrete Adjoint (First-Discretize-then-Differentiate)
Continuous Adjoint (First-Differentiate-then-Discretize).

► **Methods/software/results in this presentation rely exclusively on Continuous Adjoint.**

Part 2:

Extension of the Continuous Adjoint to Multi-Dimensional & Turbulent Flows for Shape Optimization (ShpO)- Capabilities of *adjointOptimisationFoam*! Industrial Applications

Continuous Adjoint in 2D/3D Laminar Flows- ShpO – Primal Eqs.

Laminar flow of an incompressible fluid :

$$R^p = -\frac{\partial v_j}{\partial x_j} = 0$$

$$R_i^v = \frac{\partial (v_j v_i)}{\partial x_j} - \frac{\partial \tau_{ij}}{\partial x_j} + \frac{\partial p}{\partial x_i} = 0 \ , \qquad i = 1, 2(, 3)$$

where $\tau_{ij} = \nu \left(\frac{\partial v_i}{\partial x_j} + \frac{\partial v_j}{\partial x_i} \right)$.

For turbulent flows, see next slides.

► **Steps in the development of the Continuous Adjoint Method to this flow model:**

1. **Differentiate the primal equations (PDEs) and J w.r.t. b_n.**
2. **Derive adjoint equations (field eqs. in the form of PDEs, as well as BCs).**
3. **Discretize & solve the (primal &) adjoint PDEs.**
4. **Compute grad(J), a.k.a. Sensitivity Derivatives (SDs). Ready to update b_n!**

Adjoint-based Optimization (adjointOptimisationFoam)

Define design variables b_n	⇨	Depends on the shape parametrization (in shape optimization)
Solve flow equations $\rightarrow U$	⇨	Solves the primal (flow) equations & computes the primal solution U
Compute J	⇨	J may stand for (projected) forces, moments, losses, etc
Solve adjoint equations $\rightarrow \Psi$	⇨	Solves the adjoint equations & computes the adjoint field Ψ
Compute $\delta J/\delta b_n\ (U,\Psi)$	⇨	Computes Grad(J) w.r.t. the design variables
Update design variables	⇨	Using steepest descent, CG, Quasi-Newton methods (BFGS), etc.
Update grid	⇨	Using PDE-based, Algebraic models, etc.

(After "Update grid", the loop returns to "Solve flow equations $\rightarrow U$".)

Everything is implemented within OpenFOAM v2206: No need for third-party software, external scripts, etc

Continuous Adjoint in 2D/3D Flows- ShpO - Total/Partial Derivatives

$$\frac{\delta \Phi}{\delta b_n} = \frac{\partial \Phi}{\partial b_n} + \frac{\partial \Phi}{\partial x_k}\frac{\delta x_k}{\delta b_n}$$

Grid Sensitivities

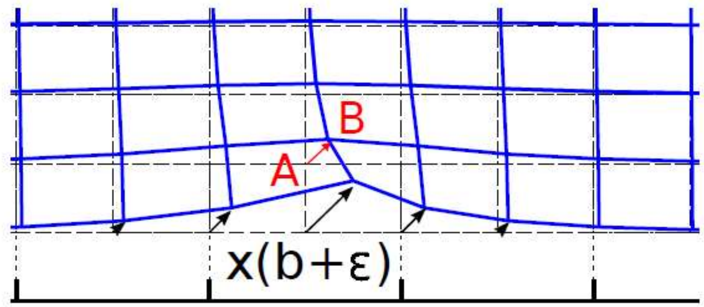

Partial (b_n) & spatial (x_k) derivatives permute!

$$\frac{\partial}{\partial b_n}\left(\frac{\partial \Phi}{\partial x_j}\right) = \frac{\partial}{\partial x_j}\left(\frac{\partial \Phi}{\partial b_n}\right)$$

Total (b_n) & spatial (x_k) derivatives don't!

$$\frac{\delta}{\delta b_n}\left(\frac{\partial \Phi}{\partial x_j}\right) = \frac{\partial}{\partial x_j}\left(\frac{\delta \Phi}{\delta b_n}\right) - \frac{\partial \Phi}{\partial x_k}\frac{\partial}{\partial x_j}\left(\frac{\delta x_k}{\delta b_n}\right)$$

The math. development of the adjoint method & the handling of Grid Sensitivities gives rise to 3 continuous adjoint formulations:

- **Field Integral (FI) Adjoint**
- **Enhanced-Surface Integral (E-SI) Adjoint**
- **Severed SI Adjoint**

The FI Adjoint Formulation (FI: Field Integral)

- **The resulting SDs include field integrals of Grid Sensitivities $\delta x_i/\delta b_n$.**

An example of such a term in the SD expression is:

$$\frac{\delta J}{\delta b_n} = \ldots + \int_\Omega \left\{ -u_i v_j \frac{\partial v_i}{\partial x_k} - u_j \frac{\partial p}{\partial x_k} - \tau^a_{ij} \frac{\partial v_i}{\partial x_k} + u_i \frac{\partial \tau_{ij}}{\partial x_k} + q \frac{\partial v_j}{\partial x_k} \right\} \frac{\partial}{\partial x_j} \left(\frac{\delta x_k}{\delta b_n} \right) d\Omega$$

Grid Sensitivities

- **Computing Grid Sensitivities requires a Grid Displacement Model (GDM) <u>& its differentiation</u> (either using finite differences, analytical differentiation, etc).**

- **SDs computed by the FI Adjoint are <u>accurate</u>; however, the cost of the part of the code dealing with grid sensitivities scales with N.**

- **Computing Sensitivity Maps using the FI Adjoint becomes prohibitively expensive, as the number of surface nodes increases.**

The E-SI Adjoint Formulation (E-SI: Enhanced Surface Integral)

- **To eliminate grid sensitivities over the domain, the Enhanced-SI (E-SI) adjoint assumes a Laplacian GDM) to be introduced into the primal equations:**

$$R_i^m = \frac{\partial^2 m_i}{\partial x_j^2} = 0$$

- **New Lagrangian & new adjoint fields (m_i^α):**

$$L = J + \int_\Omega u_i R_i^v d\Omega + \int_\Omega q R^p d\Omega + \int_\Omega m_i^a R_i^m d\Omega$$

- **Grid Sensitivities are eliminated by satisfying the adjoint GDM equations:**

$$R_k^{m^a} = \frac{\partial^2 m_k^a}{\partial x_j^2} + \frac{\partial}{\partial x_j}\left\{ u_i v_j \frac{\partial v_i}{\partial x_k} + u_j \frac{\partial p}{\partial x_k} + \tau_{ij}^a \frac{\partial v_i}{\partial x_k} - u_i \frac{\partial \tau_{ij}}{\partial x_k} - q \frac{\partial v_j}{\partial x_k} - \frac{\partial J_{\Omega'}}{\partial x_k} \right\} = 0$$

Journal of Computational Physics, 301:1-18, 2015.
Archives of Computational Methods in Engineering, 23(2): 255-299, 2016.

The E-SI Adjoint Formulation (E-SI: Enhanced Surface Integral)

- **The Enhanced-Surface Integral (E-SI) continuous adjoint method computes accurate sensitivity derivatives, with the additional advantage that the gradient of J is expressed in terms of surface integrals only ("reduced adjoint").**

- **Practically, the E-SI adjoint is as accurate as the FI adjoint, though much cheaper!**

- **What if a different (than the Laplacian) GDM is used to adapt the CFD grid to the updated geometries, during the optimization? The adjoint Laplace GDM can safely be used even in this case.**

- **A Severed-SI adjoint is also available (by arbitrarily eliminating the effect of Grid Sensitivities), though this is NOT recommended.**

Journal of Computational Physics, 301:1-18, 2015.
Archives of Computational Methods in Engineering, 23(2): 255-299, 2016.

Turbulent Flows: Continuous Adjoint & Turbulence Models

- **Enrich the Lagrangian by including the turbulence model eq(s). and the Hamilton-Jacobi eq. for computing distances from the walls (if needed). Example: Spalart-Allmaras model:**

$$L = J + \int_\Omega u_i R_i^v d\Omega + \int_\Omega q R^p d\Omega + \int_\Omega \widetilde{\nu_a} R^{\tilde{\nu}} d\Omega + \int_\Omega \Delta_a R^\Delta d\Omega$$

- **Extra adjoint equations (adjoint to the turbulence model PDEs), new terms in the adjoint mean flow eqs. and BCs.**

- **Extended to models using Wall Functions by introducing the Adjoint Wall Function.**

- **Similar developments for the adjoint to the k-ε and k-ω SST turbulence models.**

Computers & Fluids, 38:528-1538, 2009.
Journal of Computational Physics, 229(13): 5228-5245, 2010.
Archives of Computational Methods in Engineering, 23(2): 255-299, 2016.
Archives of Computational Methods in Engineering, 23(2): 255-299, 2016.

Comparison of the FI, E-SI, Severed-SI Continuous Adjoint & FD

Severed-SI Adjoint

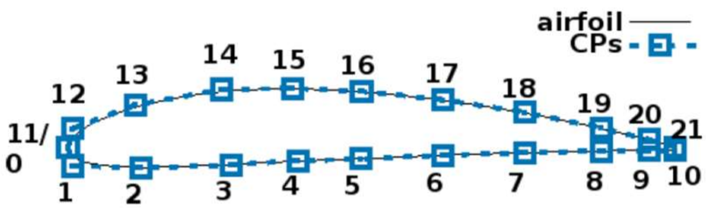

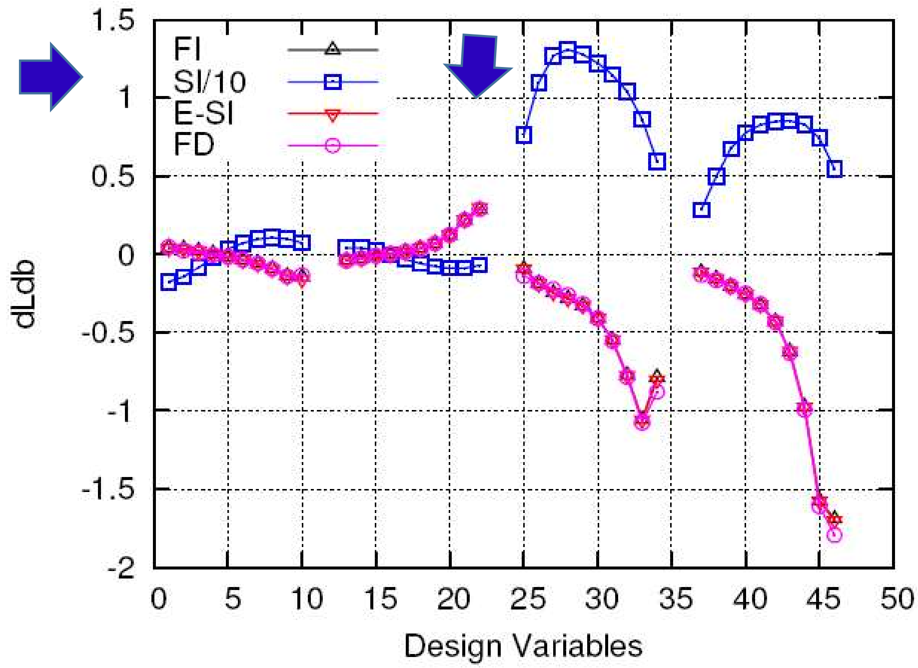

Turbulent flow around the NACA0012 airfoil ($Re=10^6$, $a_{inf}=3^o$) : Lift SDs computed by the FI, Severed-SI (scaled by 10 to fit into the same diagram), E-SI adjoint and FD. SDs computed w.r.t. the x (ID<23) and y (ID>23) coordinates of 24 NURBS CPs parameterizing the two airfoil sides. The adjoint to the Spalart-Allmaras turbulence model is used in all cases.

Why insisting on (Continuous) Adjoint to Turbulence Models?

Spalart-Allmaras Model

k-ω SST

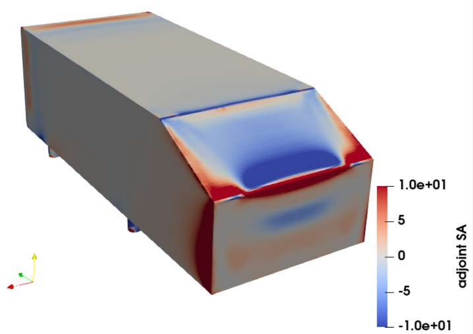

Turbulent Adjoint

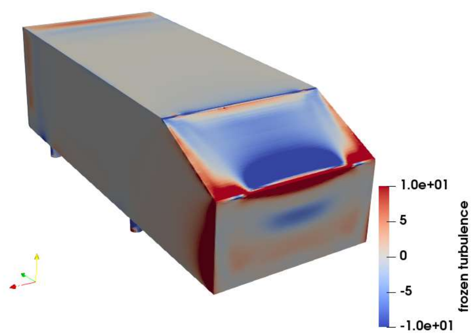

Frozen Turbulence

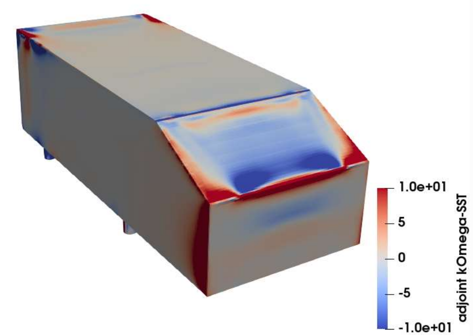

Turbulent Adjoint

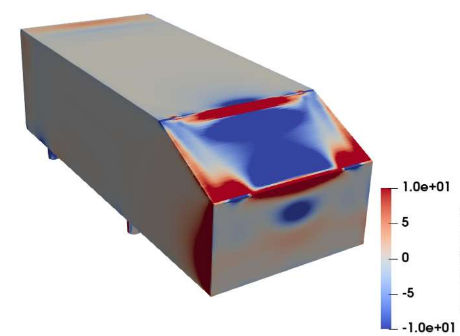

Frozen Turbulence

Drag SDs for the 2D Ahmed body (Re=2.89x10^6) computed using the adjoint to the Low-Re Spalart-Allmaras model.
The computed sensitivity maps for drag, with or without making the frozen turbulence assumption, are quite similar if the Spalart-Allmaras model is used, but noticeably differ for the k-ω STT model. In *adjointOptimisationFoam v2206* both are available. Findings confirmed with Finite Differences, not shown here.

The Volumetric B-Splines (of NURBS) Parameterization Tool

CAD-free Parameterization: Using morphing techniques based, for instance, on volumetric B-Splines. The CFD grid is adapted simultaneously with the shape to be designed. Alternatively, node-based parameterization. Returning to CAD is difficult, possibly impairing the quality of the designed shapes.

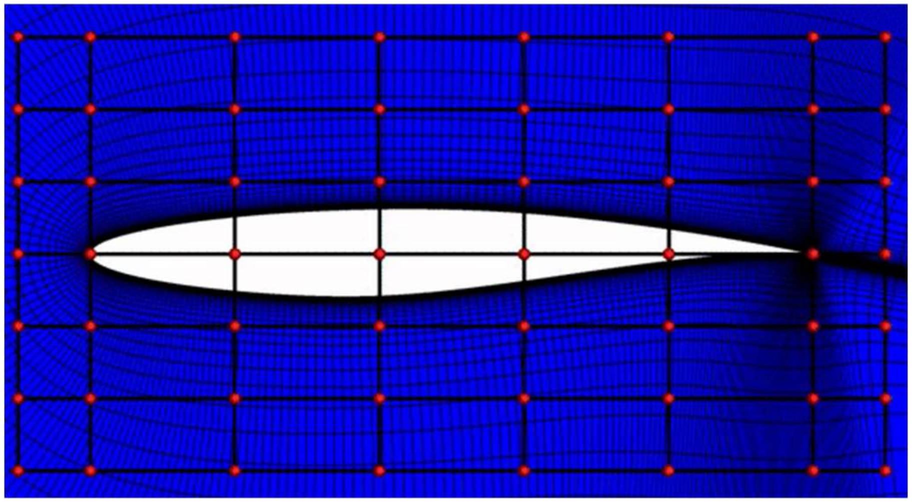

ShpO of the Side Mirror of a Car for Noise Reduction

$$J_N = \int_{\Omega'} \nu_t^2 d\Omega$$

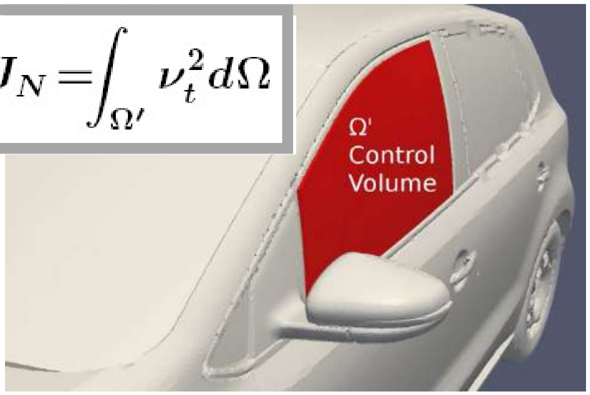

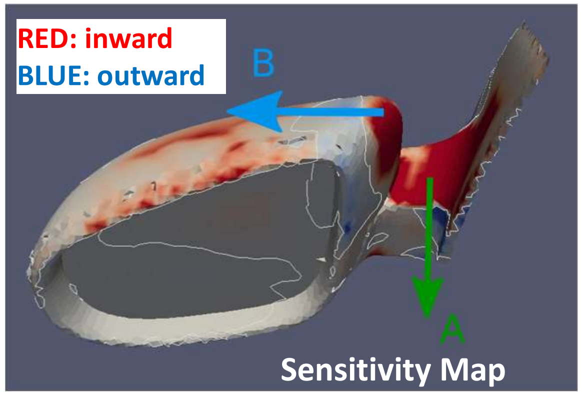

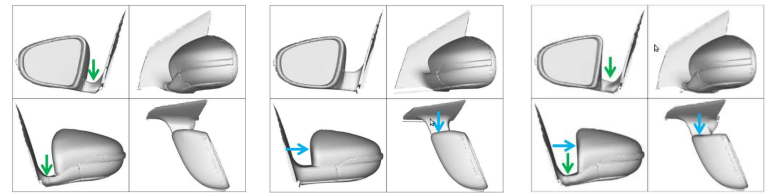

Code available in OpenFOAM v2006 onwards

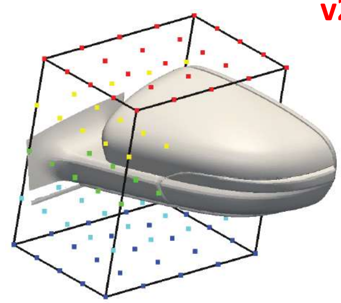

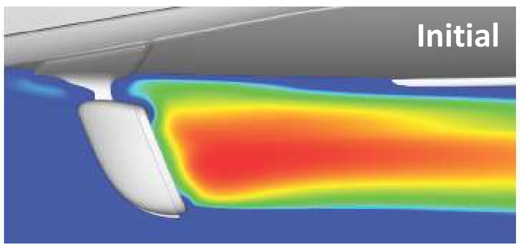

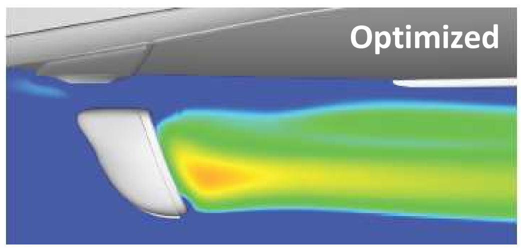

Minimization of the noise perceived by the driver. A turbulence-based objective function is used, so this problem <u>cannot</u> be solved without the adjoint to the turbulence model equations. A relatively coarse grid (2.4 Mi cells) & the Volumetric B-Splines morpher (81 DoFs) were used in the adjoint optimization. A re-evaluation of the optimal solution on a fine grid (31 Mi cells) confirmed a reduction in J_N by 25%.

Computers & Fluids, 122:223-232, 2015.

Application funded by

ShpO of the Defroster Nozzle of the HVAC unit of a Car

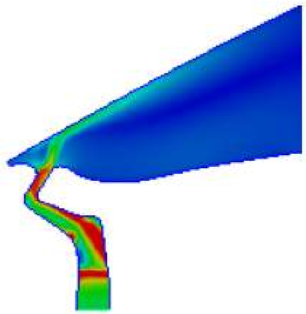

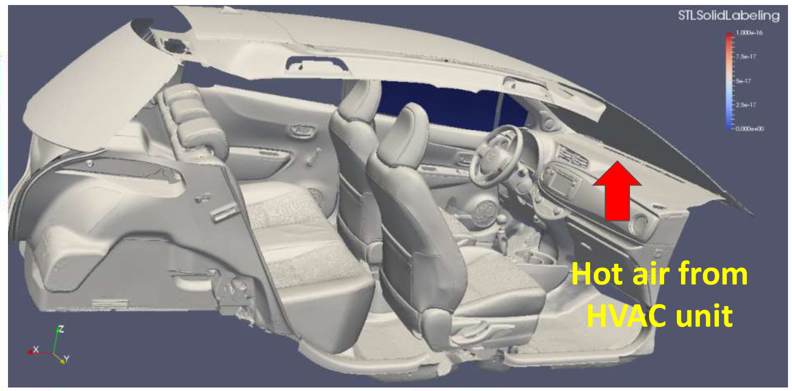

Initial   Optimized

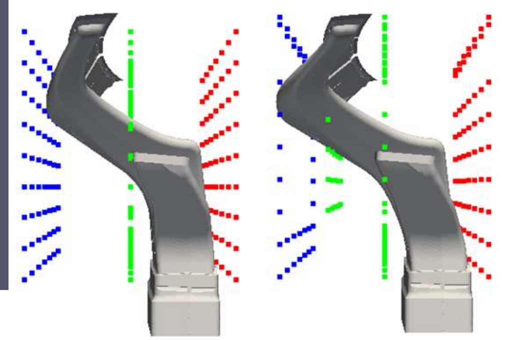

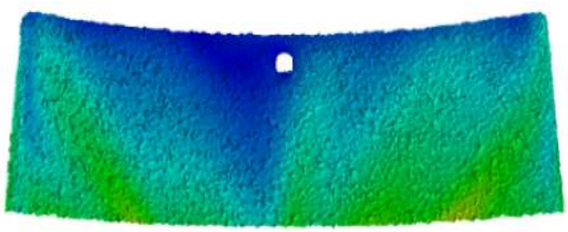

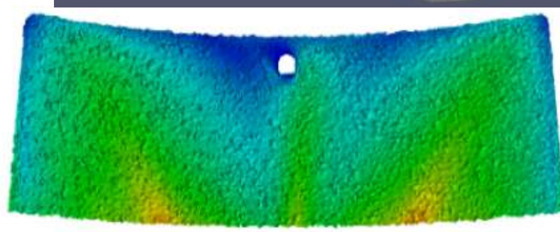

$$J_V = \frac{1}{2}\int_{\Omega'} \left(v - v^{target}\right)^2 d\Omega$$

Initial   Optimized

ShpO of the defroster nozzle of the HVAC unit of a TOYOTA passenger car, for improved defrosting/ demisting performance of the windshield. The objective was to shorten the time for dispelling condensation or frost on the windshield in the most uniform way by reaching a certain air velocity close to the windshield. The optimized geometry was manufactured (3D printing) and submitted to a defrost test in the TME's climate chamber (@ -20^o), leading to 15% less windshield defrost time.

Green areas in the velocity isolines' plot on the windshield correspond to v^{target}.

Application funded by TOYOTA

Prof. K.C. Giannakoglou, kgianna@mail.ntua.gr, Dr. E. Papoutsis-Kiachagias, vaggelisp@gmail.com

Multi-Point Aerodynamic ShpO of a Concept Car

- ShpO of an ultra-lightweight vehicle, designed by the Toyota Aerodynamic Dept., for making it less sensitive to side-wind (30^o from the port side; min. yaw moment), while maintaining a very low drag at 0^o (longitudinal wind).
- Objective function:

$$J = \omega_D C_D^{0^o} + \omega_M C_M^{30^o}$$

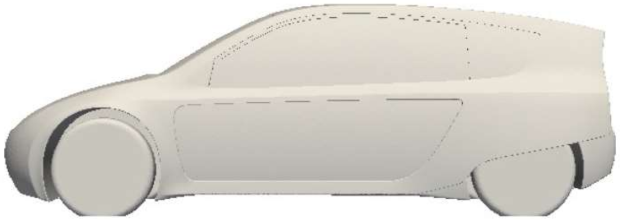

- Pareto front computed by optimizing with different values of (ω_D, ω_M).
- Two simultaneously acting morphing boxes at the spoiler and diffuser areas.
- **RANS-based adjoint optimizaton** using the adjoint to the Spalart-Allmaras model (with wall functions) & a coarse polyhedral grid with ~1.6Mi cells (average y^+=32 at the first cell-centers off the walls).

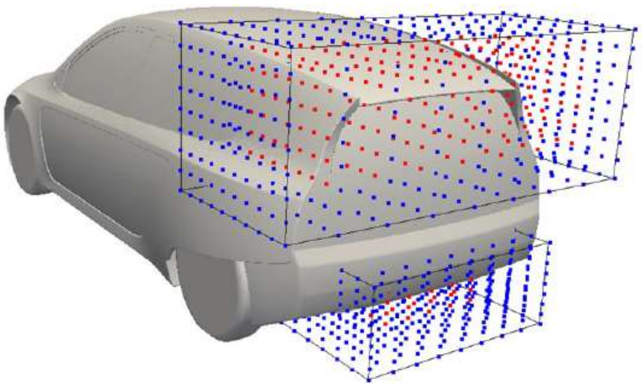

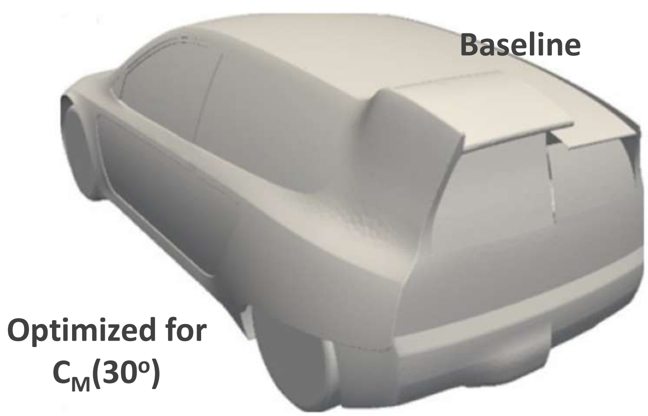

Application funded by TOYOTA

Multi-Point Aerodynamic ShpO of a Concept Car

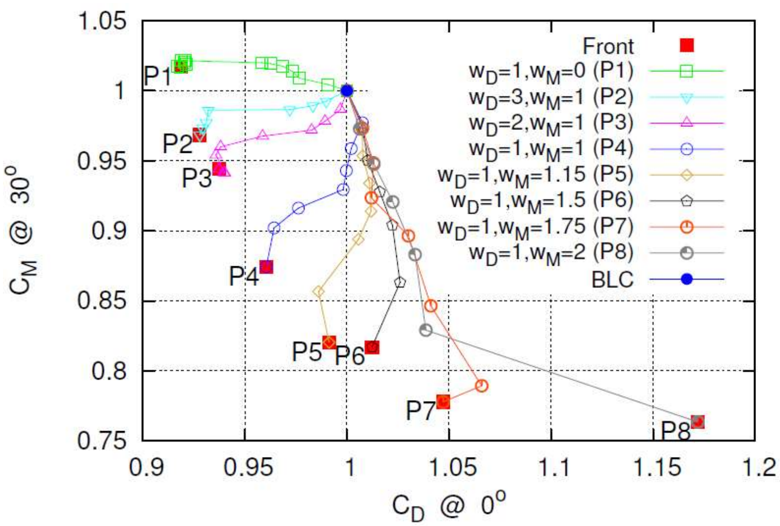

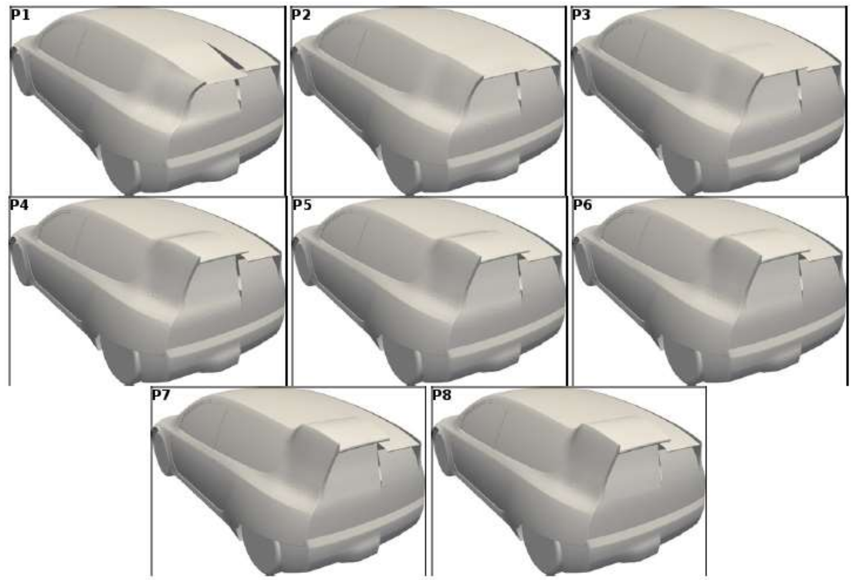

Optimized geometries (<u>port side</u>) compared to the BLC (<u>starboard side</u>). Drag reduction at 0º results from a lowered spoiler, boat-tailing and a prolonged and widened diffuser. In contrast, yaw moment reduction at 30º comes mainly from the increased spoiler height and the slight widening of the car; these increase pressure on the port side and decrease it on the starboard side to counter-balance the yaw moment of the side-wind.

Structural and Multidisciplinary Optimization, 59(2): 675–694, 2019.

Application funded by TOYOTA

Hydraulic Turbine Applications - Shape Optimization of a Francis Runner

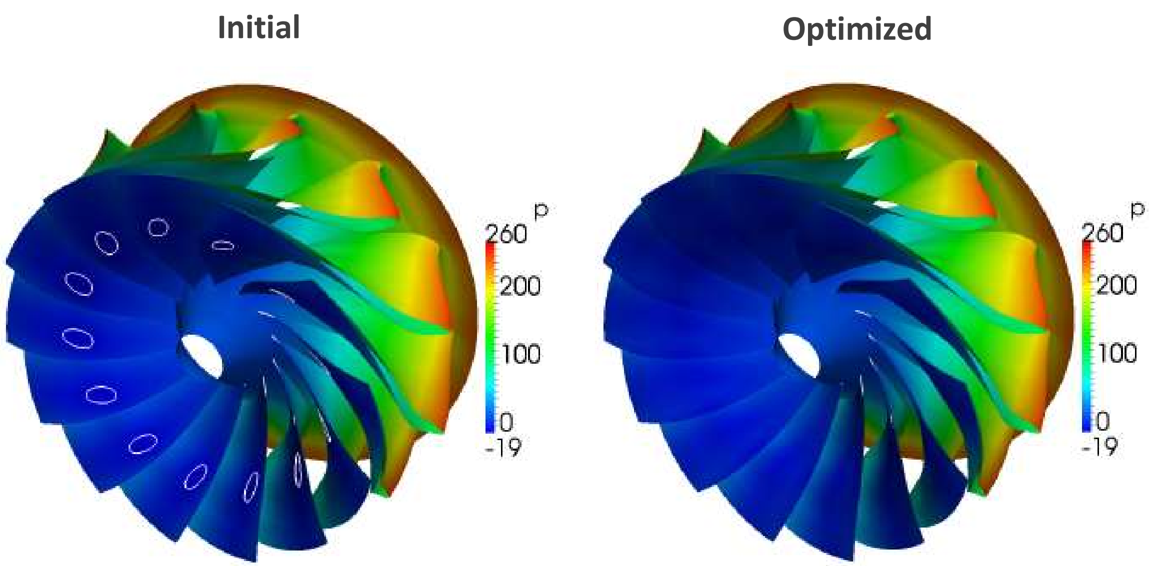

Redesigning the blades for min. cavitation. To suppress cavitation, the lowest pressure on the runner surface should become greater than the vapor pressure of the fluid. Adjoint is challenging since "min." is non-differentiable and needs to be replaced by a (differentiable) sigmoid function.

Computer Methods in Applied Mechanics and Engineering, 278:621-639, 2014.

Application funded by ANDRITZ Hydro

Part 3:
Additional Capabilities of the in-house OpenFOAM Adjoint Solver

Unsteady Adjoint: Flow Fields' Storage supported by Lossless/Lossy Compression

Lossy & Lossless compression techniques

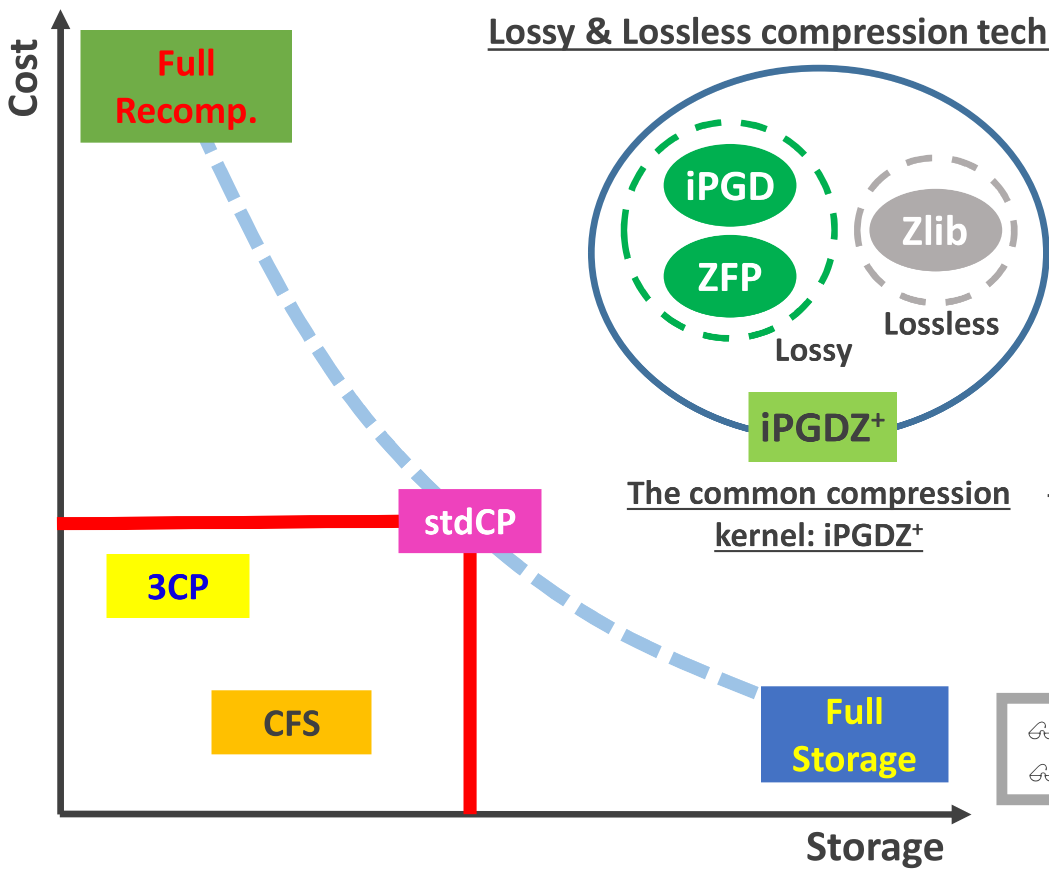

The common compression kernel: iPGDZ+

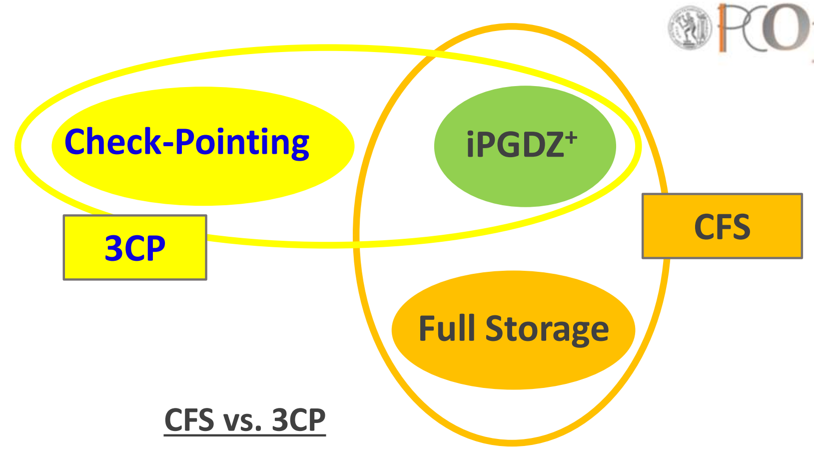

CFS vs. 3CP

Strategies for storing the flow solution time-series :

- **Compressed Full Storage (CFS)**
- **Compressed Coarse-grained Check-Pointing (3CP)**

Computer Meth. in Applied Mech. and Eng., 387: 114152, 2021.
Int. Journal of Num. Methods in Fluids, 10.1002/fld.5136, 2022.

Research funded by BMW exaFOAM

Prof. K.C. Giannakoglou, kgianna@mail.ntua.gr, Dr. E. Papoutsis-Kiachagias, vaggelisp@gmail.com

Unsteady Adjoint: ShpO of the Drivaer car for min. Drag

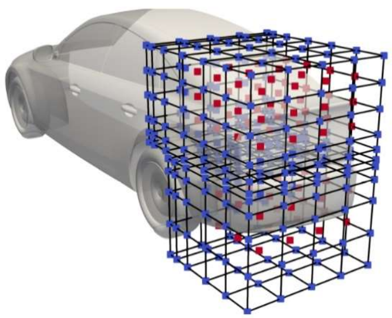

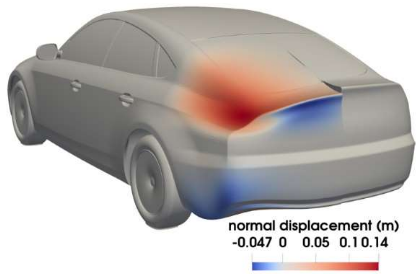

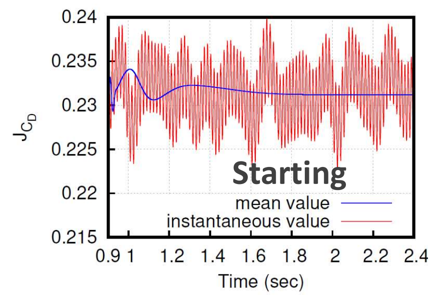

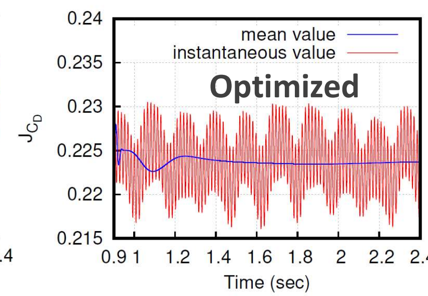

Grid: $\sim 5.3 \cdot 10^6$ cells; 40000 time-steps ($\Delta t = 6 \cdot 10^{-5} sec$)

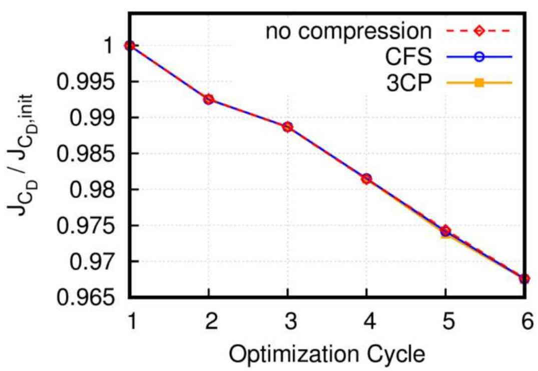

Neither CFS nor 3CP alters the convergence of the objective function!

Storage Strategy	CPU cost (%)	Compression Ratio CR	Mem (GB)	%Error in ∇J
stdCP(405)	100%	99	128*	-
CFS	71%	473	27	0.2%
3CP	94%	2240	6	0.5%

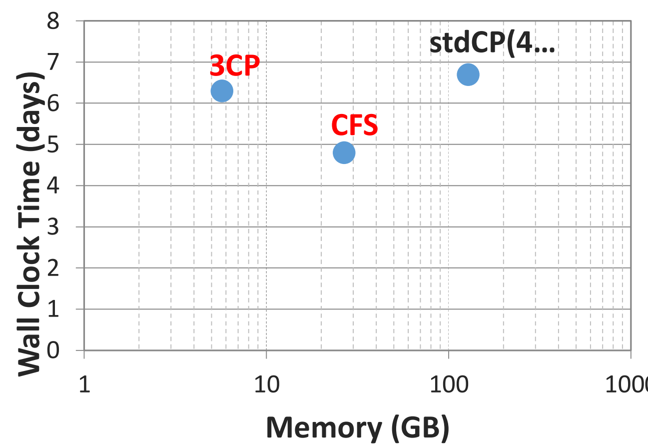

Benefits of using RPM in both Flow & Adjoint Solvers

Use of the Recursive Projection Method (RPM) to stabilize steady primal & adjoint solvers in case of convergence issues due to mild flow unsteadiness. The gain is that steady solvers can be used in the optimization.

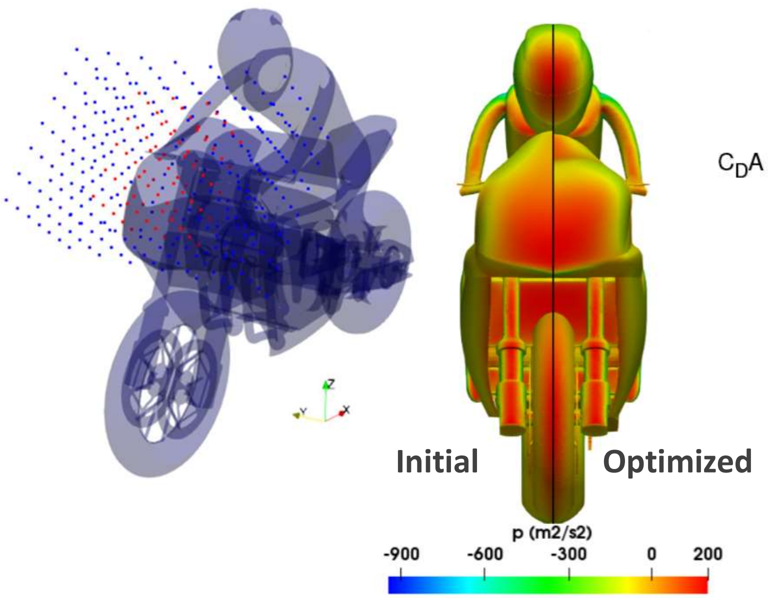

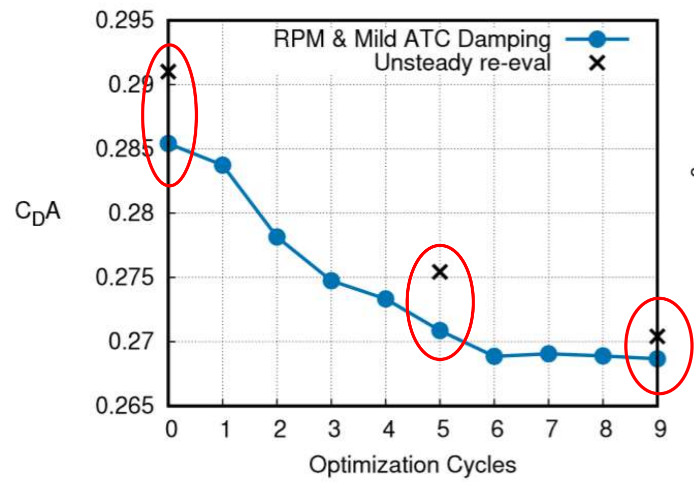

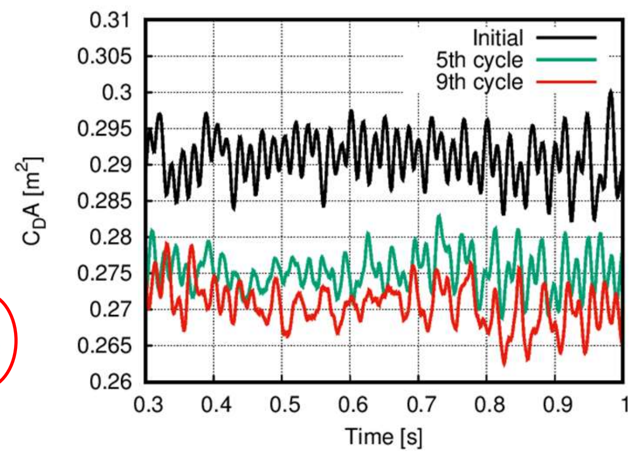

Optimization cost (on 156 cores):

- **Steady: 20h for 9 opt. cycles**
- **Unsteady: 28h for 1 flow evaluation**

Research funded by

Int J Numer Meth Fluids. 93: 2677– 2693. 2021.

Topology Optimization (TopO), even with Conjugate Heat Transfer in Bi-Fluid Devices

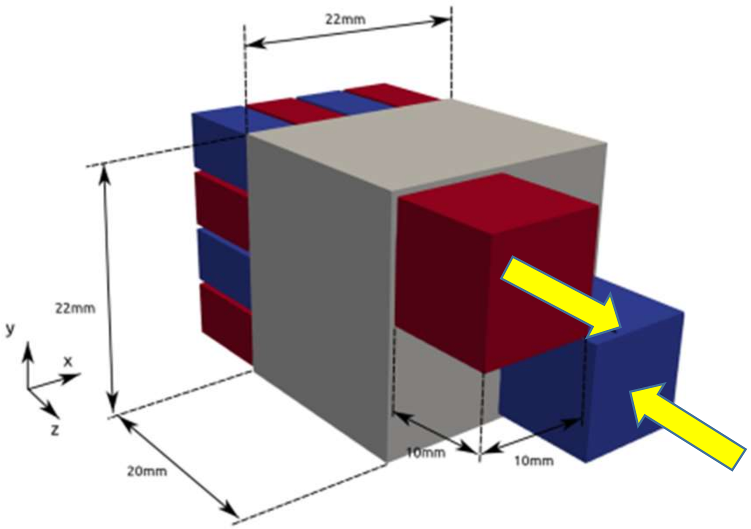

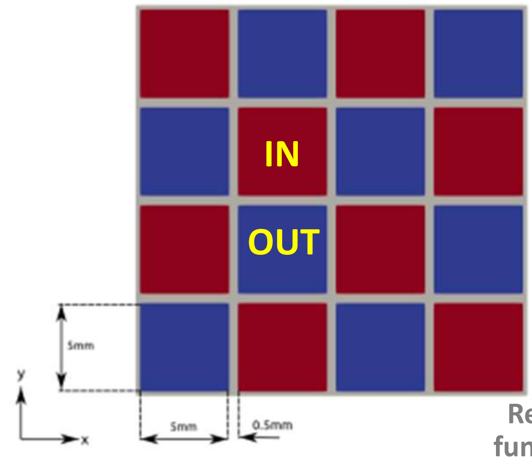

Research funded by

<u>Example:</u> Design of a compact bi-fluid counter-flow heat-exchanger with many inlets/outlets.

<u>Objectives:</u> Max. heat transfer between the cold/cold streams; also, min. total pressure losses.

<u>Constraints:</u> (1) Fluid Volumes<Threshold. (2) Equal flowrates at the 8 blue/cold exits. (3) Avoid merging the fluid streams. (4) Min. thickness of the wall separating fluid streams.

Research funded by MITSUBISHI HEAVY INDUSTRIES

TopO with CHT for the Design of a Bi-Fluid Heat Exchanger

Start with a Low-Fi TopO based on Darcy eq., easily carving the initially solid design space

$$v_i^{(\gamma)} = -\frac{1}{\beta_{max}\left(Da + I\left(\xi^{(\gamma)}\right)\right)}\frac{\partial p^{(\gamma)}}{\partial x_i}$$

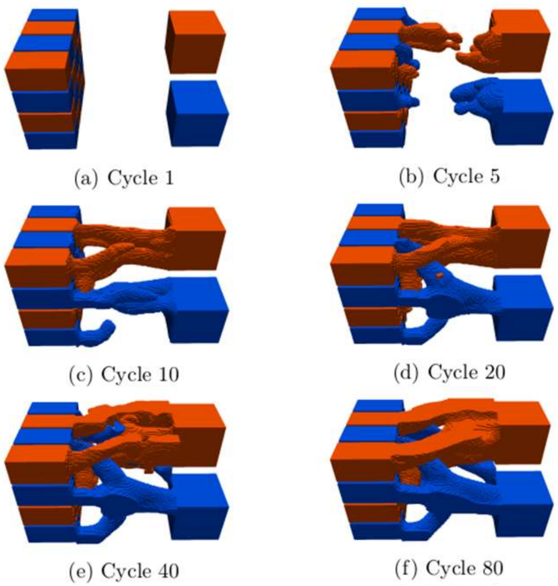

(a) Cycle 1 (b) Cycle 5 (c) Cycle 10 (d) Cycle 20 (e) Cycle 40 (f) Cycle 80

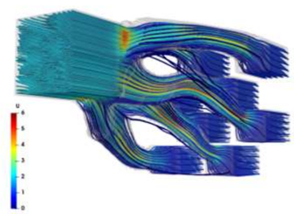

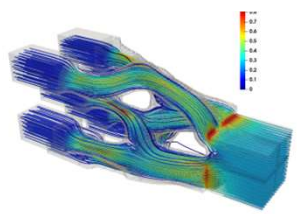

Continue with Hi-Fi TopO, based on the RANS eqs.

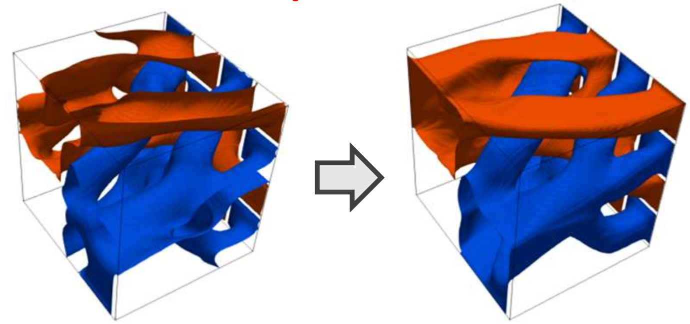

Comparison of Low-Fi & Hi-Fi TopO Solutions

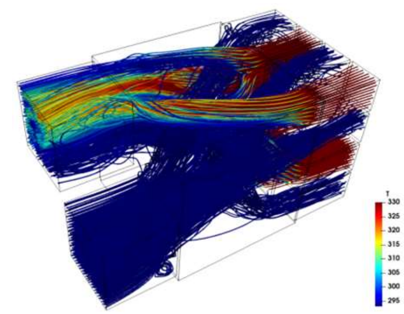

Flow in the Hi-Fi TopO Solution

Research funded by MITSUBISHI HEAVY INDUSTRIES

TopO with CHT for the Design of a Bi-Fluid Heat Exchanger

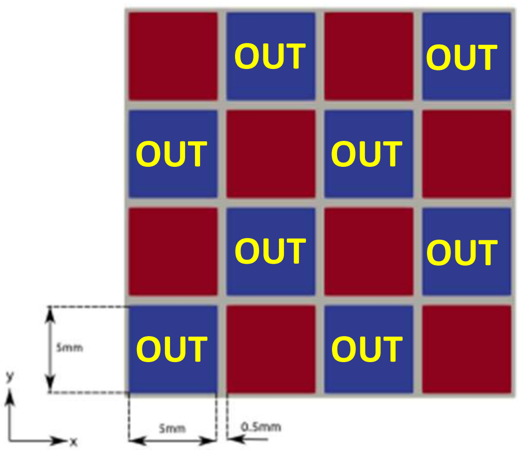

How balanced volume flow-rates at the 8 blue exits are for the Low-Fi TopO?

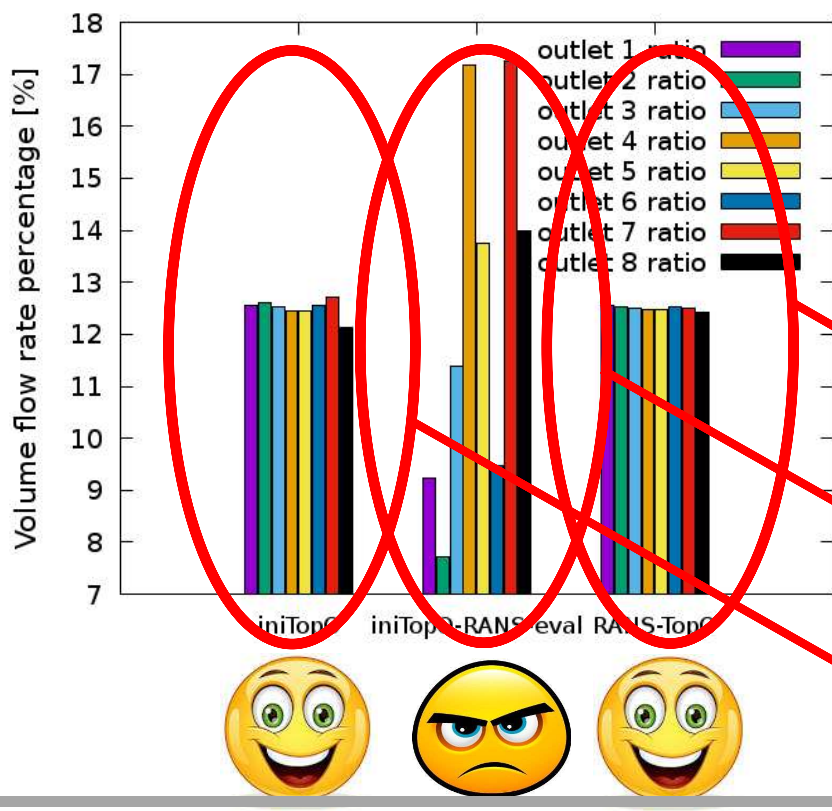

Solution of Hi-Fi TopO

Outcome of Low-Fi TopO, re-evaluated with the Hi-Fi S/W

Solution of the Low-Fi TopO

Structural and Multidisciplinary Optimization, 65(9), 245, 2022.

Research funded by MITSUBISHI HEAVY INDUSTRIES

TopO with CHT for the Design of a Bi-Fluid Heat Exchanger

Last step: A body-fitted grid is generated & CHT ShpO based on RANS is performed. This ends up with less ΔP_t by 30%, while maintaining the same amount of exchanged heat.

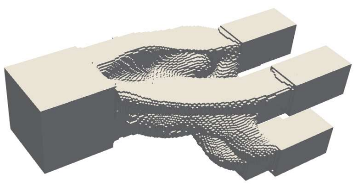

TtoST

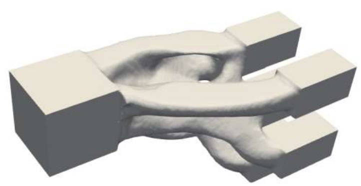

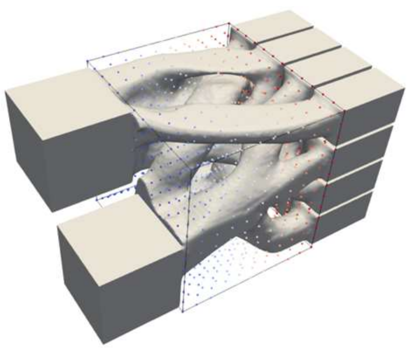

Morphing using volumetric B-Splines morphing (a single lattice of 13x13x11 control points).

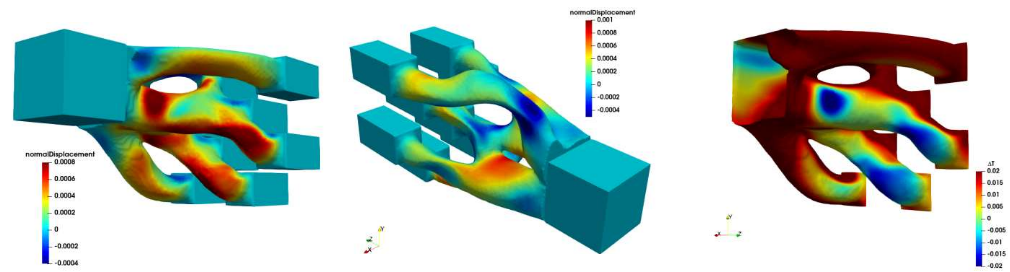

CHT ShpO Solution

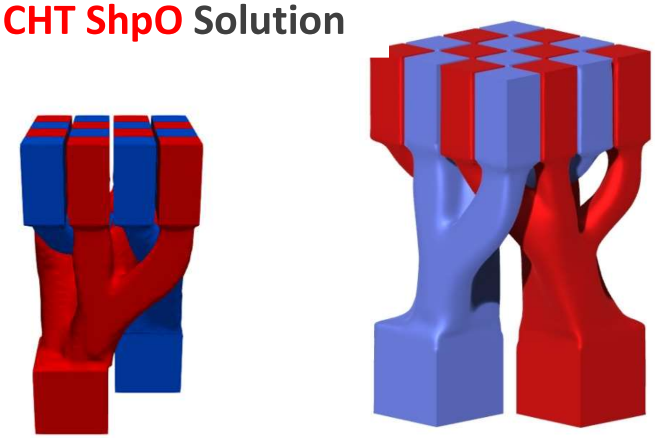

CPU Cost on 128 Intel(R) Xeon(R) CPU E5-2630 v4 @ 2.20GHz cores:

- **Low-Fi TopO**: 1h (100 cycles)
- **Hi-Fi TopO**: 9.3 hours (50 cycles)
- **CHT RANS-ShpO**: 15.5 hours (15 cycles)

Structural and Multidisciplinary Optimization, 65(9), 245, 2022.

Research funded by MITSUBISHI HEAVY INDUSTRIES

Other Topics

- **Uncertainty Quantification (UQ) based on Adjoint-Assisted Polynomial Chaos Expansion (APCE) & the Method of Moments (MoMs): First-Order Second-Moment (FOSM) & Second-Order Second-Moment (SOSM). Use of projection-based variants of FOSM & APCE, to be referred to as pFOSM & pAPCE, for gradient-based shape optimization, in the presence of uncertainties.**
- **Development of accurate discretization schemes for the continuous adjoint equations, inspired by (hand-differentiated) discrete adjoint.**

Publicly Available Tools (in OpenFOAM):

Version	Contributions
v1906	• Adjoint to the incompressible, steady-state flows • Adjoint to the Spalart-Allmaras turbulence model • Computation of sensitivity maps
v1912	• Surface/volume parameterization using volumetric B-Splines • Automated shape optimization loop
v2006	• New objective function for noise minimization
v2112	• Smoothing of sensitivity maps using a Laplace-Beltrami operator
v2206	• Adjoint to the k-ω SST turbulence model

The latest version of the software can be downloaded from
https://develop.openfoam.com/Development/openfoam
The development branch can be found in
https://develop.openfoam.com/Development/openfoam/-/tree/develop
Extensive user-guide is available at
openfoam.com/documentation/files/adjointOptimisationFoamManual_v2006.pdf

Coming Event!

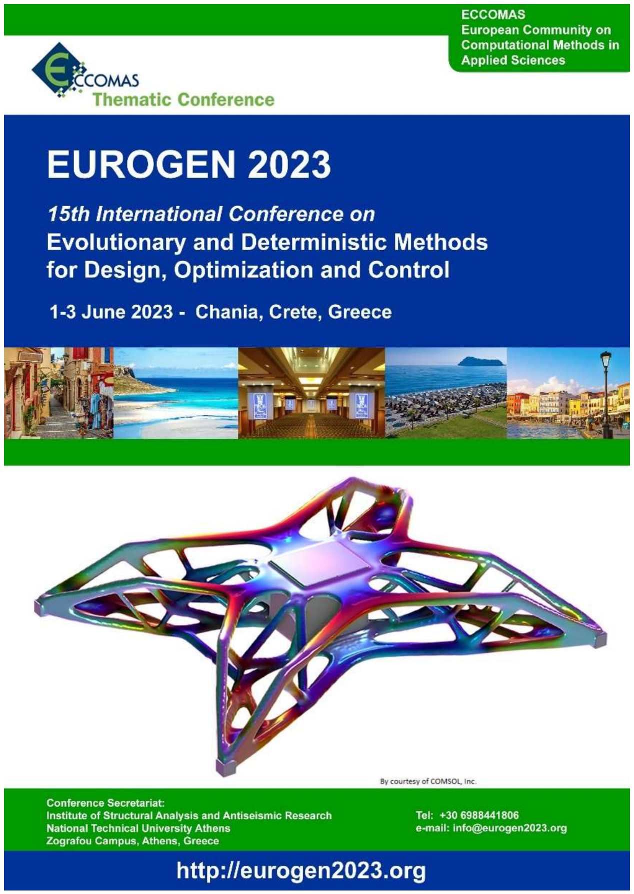

1-3 June 2023, Chania, Crete, Greece
15th International Conference on Evolutionary and Deterministic Methods for Design, Optimization and Control

An ECCOMAS Thematic Conference
EUROGEN 2023 is the **fifteenth edition** of the **Conference on Evolutionary and Deterministic Methods for Design, Optimization and Control** and one of the Thematic Conferences of the European Community on Computational Methods in Applied Sciences (ECCOMAS).

The Conference will be held at the Hotel Minoa Palace in Chania, Crete, Greece

Deadline for Abstract Submission: **5 November 2022 (but…)**